RSC Advances

PAPER

View Article Online
View Journal | View Issue

Check for updates

Cite this: *RSC Adv.*, 2020, **10**, 11816

A promising insensitive energetic material based on a fluorodinitromethyl explosophore group and 1,2,3,4-tetrahydro-1,3,5-triazine: synthesis, crystal structure and performance†

Huan Huo,[a] Junlin Zhang,[ab] Jun Dong,[a] Lianjie Zhai,[ab] Tao Guo,[a] Zijun Wang,[a] Fuqiang Bi*[ab] and Bozhou Wang *[ab]

The introduction of fluorodinitromethyl energetic groups is an efficient strategy to improve the performances of energetic materials. In this paper, an insensitive energetic compound 6-(fluorodinitromethyl)-3-nitro-1,2,3,4-tetrahydro-1,3,5-triazine (FMTNT) was designed and synthesized based on the modification of 1,3,5-triazine backbone *via* the nitration-rearrangement, reduction and fluorination sequence. The single crystal of FMTNT was firstly obtained and determined, meanwhile, this novel structure was also fully characterized by the methods of IR, ^{1}H NMR, ^{13}C NMR, ^{19}F NMR and elemental analysis. Studies on thermal behaviors and detonation performances of FMTNT were also carried out through differential scanning calorimetry (DSC-TG) approach and EXPLO5 program, respectively. The decomposition temperature of FMTNT is found to be at 157.5 °C *via* thermal chemical analysis and the detonation performances were proved to be good, with a detonation velocity of 8624.8 m s^{-1} and detonation pressure of 29.1 Gpa. Furthermore, the experimental results showed that impact and friction sensitivity reaches 20 J and 240 N, even less sensitive than TNT, indicating a broad perspective in the application of insensitive explosives and propellants.

Received 16th January 2020
Accepted 6th March 2020

DOI: 10.1039/d0ra00474j

rsc.li/rsc-advances

Open Access Article. Published on 24 March 2020. Downloaded on 5/11/2026 10:03:20 AM.
This article is licensed under a Creative Commons Attribution-NonCommercial 3.0 Unported Licence.

Introduction

The development of new explosives with high energy, lower sensitivities and good thermally stability for military application is a perennial pursued objective in the energetic materials field.[1] In most cases, further functionalization of energetic heterocyclic rings with highly oxidative explosophore groups can greatly enhance the detonation performances due to the improvement of oxygen balance. Meanwhile, the replacement of a combustible element or oxygen element of CHON compounds with larger atomic number has also been proved to be an efficient approach to promote the corresponding energetic properties.[2] In recent years, energetic materials with fluorodinitromethyl (–CF(NO$_2$)$_2$) groups have attracted intensive attentions and achieved great success, exhibiting impressive high densities and low sensitivities in rocket propellants and explosives formulations.[3] In 2019, our group also achieved two new fluorodinitromethyl-functionalized energetic materials with outstanding explosive performances (D = 9509 m s^{-1}, P = 42.6 GPa) based on trifuroxan backbones, however, their sensitivities are still too high (Fig. 1).[4]

1,1-Diamino-2,2-dinitroethene (FOX-7), a famous insensitive high explosives with attractive properties, contains a highly polarized C=C bond with two electron-donating amino groups at one carbon and two electron-withdrawing nitro groups at the other carbon, forming impressive inter and intramolecular hydrogen bonds system.[5] Since its first discovery, intensive modification reactions based on FOX-7 structure have been explored, aiming to form new insensitive backbones and leading to great success in the field of energetic materials.[6] Herein, we

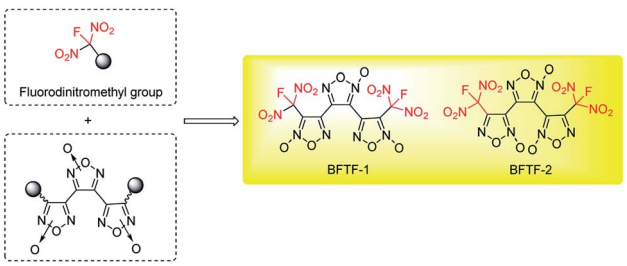

Fig. 1 Fluorodinitromethyl-functionalized energetic materials based on a trifuroxan backbone.

[a]*Xi'an Modern Chemistry Research Institute, Xi'an, 710065, China. E-mail: wbz600@163.com; bifuqiang@gmail.com*

[b]*State Key Laboratory of Fluorine & Nitrogen Chemical, Xi'an, 710065, China*

† Electronic supplementary information (ESI) available: Experimental section, X-ray crystallography of single crystals and computation details. CCDC 1908214. For ESI and crystallographic data in CIF or other electronic format see DOI: 10.1039/d0ra00474j

This journal is © The Royal Society of Chemistry 2020

Open Access Article. Published on 24 March 2020. Downloaded on 5/11/2026 10:03:20 AM.
This article is licensed under a Creative Commons Attribution-NonCommercial 3.0 Unported Licence.

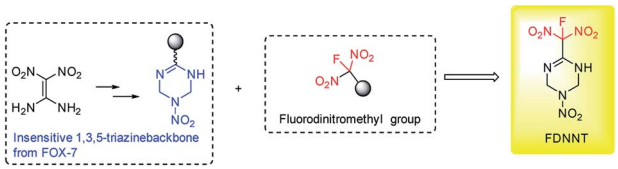

Fig. 2 Designed fluorodinitromethyl-functionalized energetic materials based on FOX-7 derived 1,3,5-triazine backbone.

reported a novel energetic materials, 6-(fluorodinitromethyl)-3-nitro-1,2,3,4-tetrahydro-1,3,5-triazine (FMTNT), constructed by introducing fluorodinitromethyl group into a FOX-7 derived insensitive 1,3,5-triazine backbone (Fig. 2). The FMTNT sample was synthesized through a nitration-rearrangement, reduction and fluorination sequence and the new structure was fully characterized by the methods of X-ray analysis, IR, ^{1}H NMR, ^{13}C NMR, ^{19}F NMR and elemental analysis. Studies on thermal behaviors and detonation performances of FMTNT were carried out through differential scanning calorimetry (DSC-TG) approach and EXPLO5 program, respectively. In addition, its mechanical sensitivities, such as impact and friction sensitivity, were obtained by test method.

Results and discussion

Synthesis and characterization towards FMTNT

The synthesis of FMTNT was based on a FOX-7 derived insensitive 1,3,5-triazine backbone (**1**), which was prepared according to literature procedures.[7] Under the HNO_3–NH_4Cl conditions, both the nitrolysis and chlorination-rearrangement processes were observed in one step with the C=C bond migrated into the cyclic skeleton, resulting a new C=N bond. A potassium salt was formed when treated the chlorodinitromethyl group with KI. Considering the existence of N–H moiety, which will also react under most of fluorination conditions, the fluorination condition need to be highly selective. After careful condition screening, the fluorodinitromethyl group was finally introduced by the addition of XeF_2 with a yield of 41% (Scheme 1). The structure of FMTNT was fully characterized by IR, ^{1}HNMR, ^{13}C NMR, ^{19}F NMR, and elemental analysis. Seen from the ^{13}C NMR spectra (Fig. 3(A)), it is clear that the resonance signals for C4 (δ = 118.90 ppm) and C3 (δ = 143.90 ppm) have been divided due to the interaction with F atom and these constants are in good agreement with their typical values.[8] ^{19}F NMR spectrum (Fig. 3(B)) showed the resonance signal of FMTNT is at −101.87 ppm, which is comparable with the δ value of some known compounds.[9]

The crystal sample of FMTNT was grown in a mixture of ethyl acetate/hexane and its crystal structure was determined by X-ray single-crystal diffraction at room temperatures, with the data and parameters of the X-ray measurements and structure refinements given in Table 1. FMTNT crystallized in the $P_2(1)/c$ space group with molecules in the unit cell (Fig. 4) and the crystal density is 1.761 g cm^{-3}. The molecular structure of FMTNT is composed of a branched 1,2,3,4-tetrahydro-1,3,5-triazine with a fluorodinitromethyl group attached to C(2) and a nitro group attached to N(5). All of the bond distances are well within the normal range and listed in Table S1 in the ESI.† The length of the C–NO_2[N(1)–C(1), N(2)–C(1)] joining the fluorodinitromethyl group are 1.539(8) Å and 1.527(8) Å, respectively, and longer than that of F(1)–C(1) (1.400(7) Å), which indicates that compared with C–F of fluorodinitromethyl, C–NO_2 breaks will be easier.

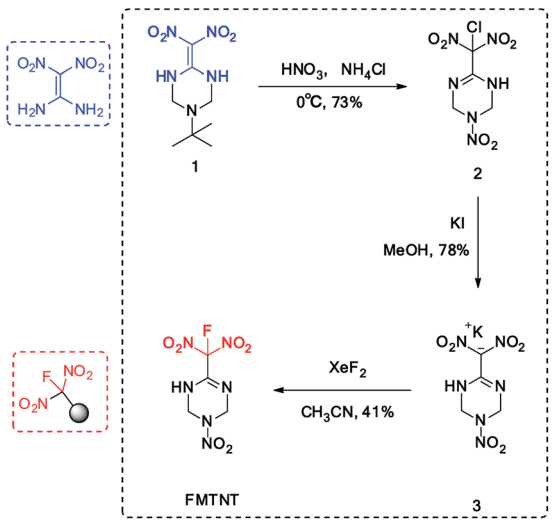

Scheme 1 Synthetic route towards FMTNT.

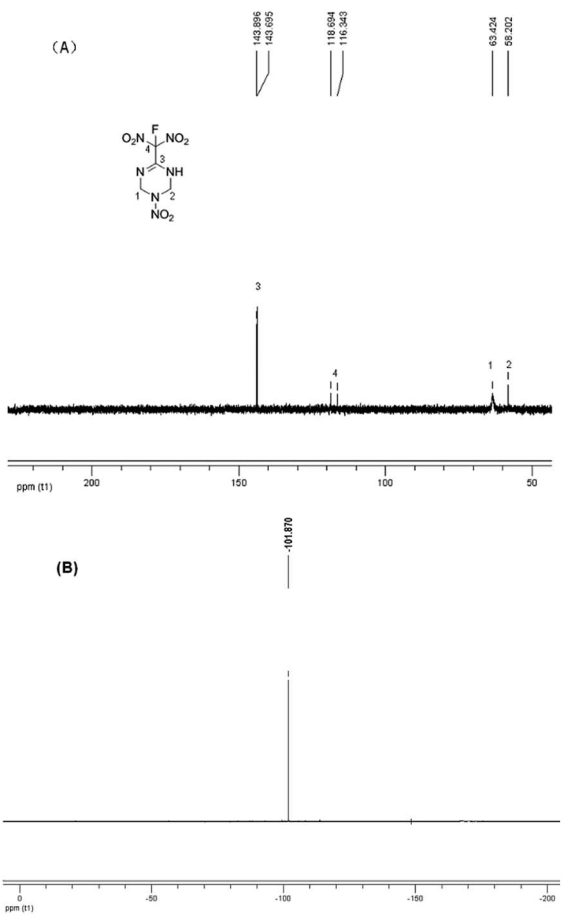

Fig. 3 ^{13}C NMR spectrum (A) and ^{19}F NMR spectrum (B) of FMTNT.

Open Access Article. Published on 24 March 2020. Downloaded on 5/11/2026 10:03:20 AM.
This article is licensed under a Creative Commons Attribution-NonCommercial 3.0 Unported Licence.

Table 1 Crystallographic details of FMTNT

Compd	FMTNT
Formula	$C_4H_5FN_6O_6$
Formula weight	252.14
T (K)	296(2)
λ (Å)	0.71073
Crystal system	Monoclinic
Space group	$P_2(1)/c$
a (Å)	11.592 (14)
b (Å)	8.138 (10)
c (Å)	11.045 (14)
Volume (Å^3)	951 (2)
Z	4
D_c (g cm^{-3})	1.761
F (000)	512
θ range/(°)	1.92 to 25.10
Reflections collected/unique	4464/1693 [$R_{(int)} = 0.1367$]
Refinement method	Full-matrix least-squares on F^2
GOF on F^2	0.949
Final R indexes ($I > 2\sigma(I)$)	$R_1 = 0.0751$, w$R_2 = 0.1752$
Final R indexes (all data)	$R_1 = 0.1924$, w$R_2 = 0.2415$
Largest diff peak and hole (e Å^{-3})	0.328 and −0.349
GOF on F_2	0.949
CCDC number	1908214

Moreover, the C=N double bond (N(4)–C(2) 1.271(7) Å) length of 1,2,3,4-tetrahydro-1,3,5-triazine is found between the bond lengths of a C–N single bond (1.47 Å) and a C=N double bond (1.22 Å).[10] The N(5)–N(6) bond length (1.394(7) Å) is shorter than the normal N–N single bond (1.450 Å). The average N–O bond length of all nitro groups in fluorodinitromethyl moiety is 1.207(7) Å, which is similar to that of the trinitromethyl group (1.209 Å). The bond angle of F(1)–C(1)–N(1) and F(1)–C(1)–N(2) are all uniform (107.6(5)°), showing that the angle between the F atom and the two nitro groups is essentially the same, and both to be perpendicular. Furthermore, the fluorodinitromethyl group is out of the plane of the 1,2,3,4-tetrahydro-1,3,5-triazine ring, and will not show the propeller-like conformation any more, with C1–C2–N–O torsion angles (O(4)–N(2)–C(1)–C(2) −83.0 (7)°, O(3)–N(2)–C(1)–C(2) −94.2 (7)°, O(1)–N(1)–C(1)–C(2) −13.1 (8)° and O(2)–N(1)–C(1)–C(2) 166.3(6)°) which are not in the typical range for the propeller-like structure (23–67°) as described in the literature.[11]

Hirshfeld surfaces are widely used to identify and quantify the interaction nature and proportion in crystals. In Fig. 5,

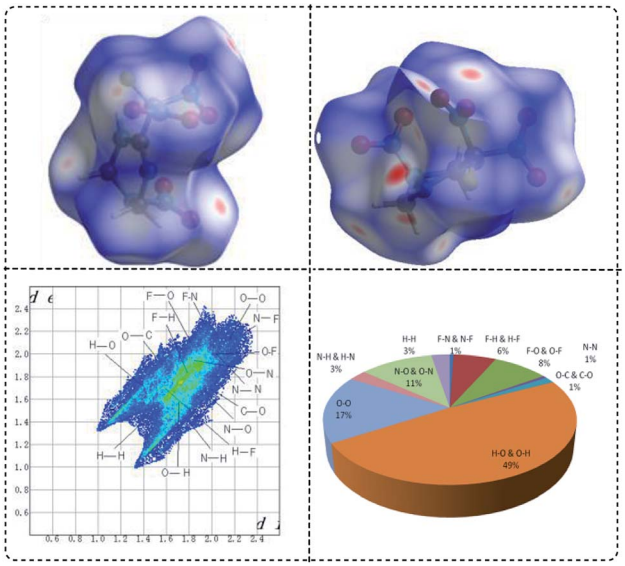

Fig. 5 Hirshfeld surfaces calculation (white, distance d equals the van der Waals distance; blue, d exceeds the van der Waals distance; red, d is less than van der Waals distance) and two-dimensional (2D)-fingerprint plots of FMTNT.

Hirshfeld surfaces, fingerprint plots and crystal packing diagrams of FMTNT are showed respectively. As demonstrated, the two dimensional (2D)-fingerprint of crystals FMTNT and the associated Hirshfeld surfaces were employed to show their intermolecular interactions. The red and blue regions on the Hirshfeld surfaces represent high and low close contact

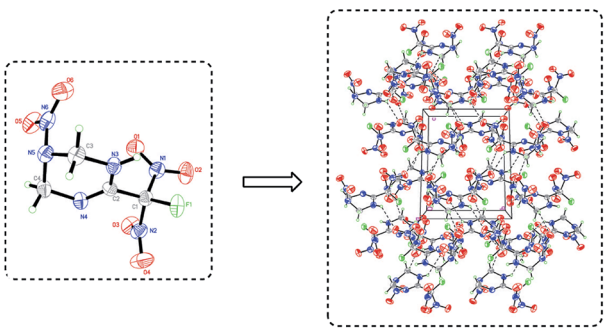

Fig. 4 Molecular structure of FMTNT and its view of crystal packing down the c axis.

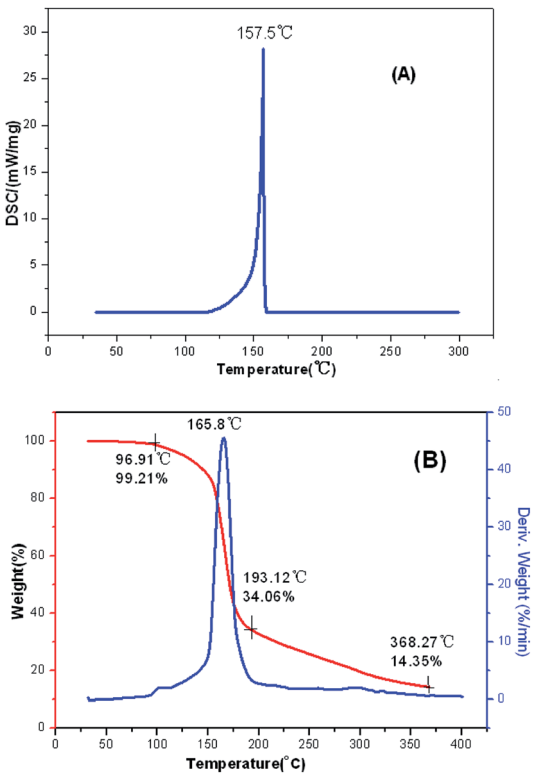

Fig. 6 DSC curve (A) and TG-DTG curve (B) of FMTNT.

This journal is © The Royal Society of Chemistry 2020

Open Access Article. Published on 24 March 2020. Downloaded on 5/11/2026 10:03:20 AM.
This article is licensed under a Creative Commons Attribution-NonCommercial 3.0 Unported Licence.

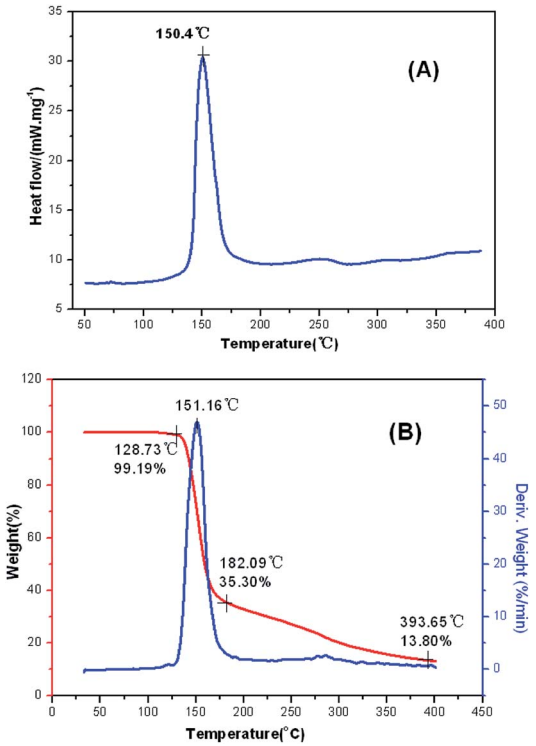

Fig. 7 DSC curve (A) and TG-DTG curve (B) of **2**.

populations, respectively. FMTNT appear as uneven blocks with dots dispersed in many orientations. Red dots denotes the intermolecular C–H···O and N–H···O interactions. Other areas on the surfaces usually belong to O···O, C···O and N···O interactions. This can also be confirmed by regular 2D and decomposed 2D fingerprint plots, O···H close contacts are the dominant interaction. The percentage of O···H close constants is near 50%, suggesting hydrogen bonds are important characteristics of FMTNT, which should ensure stability and insensitivity.

Studies on thermal behaviors and electrostatic potentials (ESPs) of the FMTNT

The main text of the article should appear here with headings as appropriate. The thermal behaviors of FMTNT and compound **2** were studied by TG-DSC method (Fig. 6 and 7). According to DSC-TG experiments, FMTNT and its similar structure compound **2** showed only one thermal decomposition peak temperature at 157.5 °C and 150.4 °C under the heating rate of 10 °C min^{-1}, respectively. For FMTNT and compound **2**, there is one decomposition processes with the DTG peaks from 96.91 to 193.12 °C, and 128.73 to 182.09 °C, the total weight loss is 65.15% and 64.70%, respectively. The result indicates that there are a few remains at the end of the decomposition.

The electrostatic potentials (ESP) of the FMTNT molecular surfaces were calculated by the B3LYP/6-311++g(d, p) basis set with the optimized structure, and defined as 0.001 electron per bohr. Fig. 8 shows the ESP of the electron density evaluated at the B3LYP level of theory. The area and strength of the positive and negative electrostatic potentials region are statistically

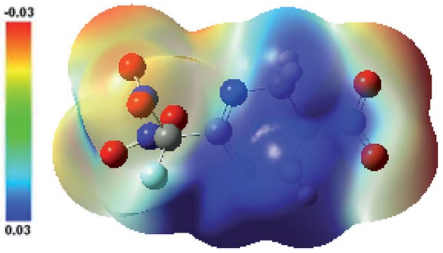

Fig. 8 Electrostatic potentials distribution of FMTNT.

analyzed by the Multiwfn program,[12] and the results are listed in Table 2. According to Klapötke,[13] in the energetic system, the surface area and the strength of the electropositive potential surfaces are related to the impact sensitivities, and the surface area of the positive charge is larger, and the intensity is greater than the negative electrostatic potentials area. In Fig. 8, it can be clearly seen that the negative ESP region of FMTNT is smaller and also a lower charge separation; the Table 2 shows, the positive ESP area of FMTNT is larger than the negative ESP area, and its ratio is 1.0324; otherwise, the strength of the positive ESP reached about twice the strength of negative ESP.

Studies on detonation properties of the FMTNT

Studies on detonation properties of the FMTNT was carried out through quantum computations methods with the Gaussian 09 (Revision A. 02) suite of programs.[14] The optimized structures were characterized to be true local energy minima on the potential-energy surface without imaginary frequencies. The gas phase heats of formation were calculated by the atomization method using the Gaussian 09 program package at the CBS-4M level of theory.[15] Gas phase heat of formation was transformed to solid phase heat of formation by Trouton'srule.[16] Based on the crystal density and calculated heat of formation, the detonation velocity and detonation pressure for FMTNT was calculated by EXPLO5 6.04.[17] The sensitivities towards impact and friction for FMTNT was measured and evaluated by using the standard BAM method,[18] and the predicted performance data were summarized in Table 3. It can be seen that FMTNT ($I_S = 20$ J; $F_S = 240$ N) is less sensitive than TNT ($I_S = 15$ J; $F_S = 240$ N) and compound **2** ($I_S = 10$ J; $F_S = 180$ N). Therefore, this fluorodinitromethyl compound was classified as insensitive and less sensitive energetic

Table 2 ESPs parameter of FMTNT[a]

Compd	FMTNT
A/Å^2	225.6075
A^+/Å^2	114.6023
A^-/Å^2	111.0052
A^+/A^-	1.0324
V_s^+/(kcal mol^{-1})	20.4765
V_s^-/(kcal mol^{-1})	−11.7403

[a] A the total surface area; A^+ the surface area of the positive charge; A^- the surface area of the negative charge; V_s^+ the strength of the electrostatic potential in the positive charge region; V_s^- the strength of the electrostatic potential in the negative charge region.

Open Access Article. Published on 24 March 2020. Downloaded on 5/11/2026 10:03:20 AM.
This article is licensed under a Creative Commons Attribution-NonCommercial 3.0 Unported Licence.

Table 3 Physico-chemical properties and detonation parameters of the energetic compounds

Compd	ρ^a [g cm^{-3}]	ΔH_f^b [kJ mol^{-1}]	T_d^c [°C]	D^d [m s^{-1}]	P^e [Gpa]	I_S^f [J]	F_S^g [N]
RDX[h]	1.80	92.6	204	8795	34.9	7.5	120
TNT[i]	1.65	−295.0	295	6881	19.5	15	240
BFTF-1[j]	2.00	390.1	116	9509	42.6	5	70
BFTF-2[j]	1.91	383.9	136	9196	38.8	6.5	110
2[k]	1.849	40.5	152	8192	29.5	10	180
FMTNT	1.76	3.0	157.5	8624	29.1	20	240

[a] Crystal density. [b] Calculated molar enthalpy of formation. [c] Decomposition temperature by DSC method under N_2 atmosphere with a heating rate of 10 °C min^{-1}. [d] Calculated detonation velocities. [e] Calculated detonation pressure. [f] Impact sensitivity. [g] Friction sensitivity. [h] Ref. 19. [i] Ref. 20. [j] Ref. 4. [k] Ref. 6.

materials. The properties of FMTNT were obtained by calculation or test as follows: heat of formation is 3 kJ mol^{-1}, detonation velocity and detonation pressure is 8624 m s^{-1} and 29.1 GPa, respectively. The compound FMTNT exhibits good detonation properties which is similar to RDX and higer than compound **2**. Compared with our previously reported highly energetic structures of BFTF-1 and BFTF-2, which are based on trifuroxan backbones, FMTNT exhibits much better insensitivities due to the insensitive 1,3,5-triazine backbone.

Conclusions

In summary, a new and insensitive energetic material, FMTNT, was designed and synthesized for the first time with the combination of fluorodinitromethyl group and FOX-7 derived insensitive 1,3,5-triazine backbone. Its novel structure was fully confirmed by NMR, IR, elemental analysis and single crystal X-ray diffraction, in the same time, the thermal properties investigated by DSC-TG method showed a major decomposition peak temperature of 157.5 °C. Additionally, for FMTNT, the physical and energetic properties were studied by calculated and experimental methods. According to the impact and friction sensitivity tests by using standard BAM methods, FMTNT ($I_S = 20$ J; $F_S = 240$ N) is less sensitive than TNT ($I_S = 15$ J; $F_S = 240$ N). The calculated detonation velocities and pressures of FMTNT ($D =$ 8624.8 m s^{-1}, $P = 29.1$ GPa) is comparable with those of RDX. The good detonation properties and low sensitive of these compounds indicated that this class of FMTNT is an ideal candidate as insensitive energetic materials.

Experimental section

Caution! Most compounds in this studies are energetic materials and standard safety precautions (including leather gloves, face shield and ear plugs) should be applied when the synthetic work are carried out.

Reagents and sample preparation

Hexahydro-3-*tert*-butyl-2,2-dinitromethylene-1,3,5-triazine (**1**) as a starting material was prepared according to the literature.[7] All reagents and solvents were purchased from Aladdin Bio-Chem Technology Co., Ltd (Shanghai, China) and were used without further purification unless otherwise indicated.

Apparatus and measurements

Infrared spectra were measured by an EQUINOX 55 Fourier transform infrared spectrometer (Bruker, Germany) in the range of 4000–400 cm^{-1}. ^{13}C NMR and ^{1}H NMR spectra were measured with AV 500 NMR spectrometer (Bruker, Switzerland). Elemental analyses were performed with the vario EL cube elemental analyzer (Elementar, Germany).

The thermal analysis experiment and the glass transition temperature (T_g) were performed with a model TG-DSC STA 499 F3 instrument (NETZSCH, Germany). Single crystal X-ray experiment was carried out on a Bruker Apex II CCD diffractometer equipped with graphite monochromatized Mo Kα radiation ($\lambda =$ 0.71073 Å) using ω and φ scan mode. Structures were solved by the direct method using SHELXTL and refined by means of full-matrix least-squares procedures on F^2 with the programs SHELXL-97. All nonhydrogen atoms were refined with anisotropic displacement parameters. The sensitivity towards impact (I_S) and friction (F_S) were determined according to BAM standards.

Computational details

All quantum chemical calculations were carried out using the Gaussian 09 (Revision A.02) program package and visualized by GaussView 5.08.[21] The enthalpies ($H°$) and free energies ($G°$) were calculated using the complete basis set method (CBS-4M) based on X-ray diffraction data, in order to obtain accurate. The enthalpies of the gas-phase species were estimated according to the atomization energy method.[22] The solid state enthalpy of formation can be estimated by subtracting the heats of sublimation from gas phase heats of formation. The heat of sublimation can be estimated with Trouton's rule according to eqn (1), where T represents either the melting point or the decomposition temperature when no melting occurs prior to decomposition:

$$\Delta H_{sub} = 188/\text{J mol}^{-1}\,\text{K}^{-1} \times T \quad (1)$$

 This journal is © The Royal Society of Chemistry 2020

Open Access Article. Published on 24 March 2020. Downloaded on 5/11/2026 10:03:20 AM.
This article is licensed under a Creative Commons Attribution-NonCommercial 3.0 Unported Licence.

Syntheses

Compound (2). Fuming HNO_3 (d = 1.5 g cm^{-3}, 90 mL) was added in a 250 mL round-bottom flask immersed in an ice bath, **1** (15.0 g, 61.2 mmol) was added slowly to the solution at the temperature of 0–5 °C. After the addition was complete, NH_4Cl (2.2 g, 41.1 mmol) was added over 1 h at the same temperature. The reaction mixture was stirred for 4 h and warmed to room temperature, and then poured into ice water with stirring for 1 h, the obtained precipitate was filtered off, washed with ice water, and air-dried to obtain 12.0 g solid (yield: 73.2%). IR (KBr), ν (cm^{-1}): 3423, 1294 (–NH), 3050, 2988 (–CH_2), 1651 (C=N), 1559, 1390 (–NO_2), 1032 (C–Cl); ^{1}H NMR (DMSO-d_6, 500 MHz), δ: 8.897 (s, 1H, NH), 5.512 (s, 2H, CH), 5.266 (s, 2H, CH); ^{13}C NMR (DMSO-d_6, 125 MHz), δ: 146.903 (C–Cl(NO_2)$_2$), 120.263 (C=N), 63.574 (CH_2), 56.705 (CH_2); elemental analysis (%) calcd for $C_4H_5ClN_6O_6$: C, 17.89; H, 1.88; N, 31.29; found: C, 17.99; H, 2.05; N, 31.59.

Compound (3). A solution of KI (5.6 g, 33.7 mmol) in methanol (45 mL) was stirred at room temperature and treated by dropwise addition of **2** (4.5 g, 16.8 mmol) solution in 45 mL methanol. The reaction mixture was stirred at the same temperature for 1 h. The obtained precipitate was filtered off, washed with methanol and anhydrous ether, and air-dried to obtain 3.6 g solid (yield: 78.8%). IR (KBr), ν (cm^{-1}): 3335, 1246 (N–H), 2918, 2879 (–CH_2–), 1670 (C=N), 1538, 1354 (–NO_2); ^{1}HNMR (DMSO-d_6, 500 MHz), δ: 7.684 (s, 1H, NH), 5.532 (s, 2H, CH), 5.208 (s, 2H, CH); ^{13}C NMR (DMSO-d_6, 125 MHz), δ: 148.922 (C–Cl(NO_2)$_2$), 130.804 (C=N), 59.672 (CH_2), 53.576 (CH_2); elemental analysis (%) calcd for $C_4H_6N_6O_6$: C, 17.65; H, 1.85; N, 30.87; found: C, 17.32; H, 2.01; N, 30.72.

6-(Fluorodinitromethyl)-3-nitro-1,2,3,4-tetrahydro-1,3,5-triazine (FMTNT). A solution of **3** (3.0 g, 12.8 mmol) in anhydrous acetonitrile (30 mL) was stirred at 20 °C and treated by addition of XeF_2 (4.35 g, 25.65 mmol). The reaction mixture was stirred at the same temperature for 48 h. The solvent was removed by evaporation at reduced pressure and the residue was washed to give a colorless solid. The residue was adequately dissolved with anhydrous ether. The solvent was filtered and the filtrate was concentrated in vacuum to obtain 1.35 g title compound (yield: 41.8%). IR (KBr), ν (cm^{-1}): 3386, 1267 (N–H), 3052, 2966, 2914 (CH_2), 1669 (C=N), 1600, 1564, 1540, 1353 (–NO_2), 1152 (C–F); ^{1}HNMR (DMSO-d_6, 500 MHz), δ: 9.174 (1H, NH), 5.499 (2H, CH_2), 5.320 (2H, CH_2). ^{13}C NMR (DMSO-d_6, 125 MHz), δ: 143.896 (C–F(NO_2)$_2$), 118.894 (C=N), 63.488 (CH_2), 58.202 (CH_2); ^{19}F NMR (DMSO-d_6, 470.5 MHz), δ: −101.872; elemental analysis (%) calcd. for $C_4H_5FN_6O_6$: C, 19.06, H, 2.00, N, 33.33; found: C, 19.03, H, 2.34, N, 32.92.

Conflicts of interest

There are no conflicts to declare.

Acknowledgements

We are grateful to the financial support from the National Natural Science Foundation of China (No. 21805223) and the China Postdoctoral Science Foundation (No. 2018M633552).

Notes and references

1 A. F. Baxter, I. Martin, K. O. Christe and R. Haiges, *J. Am. Chem. Soc.*, 2018, **140**, 15089; Q. Xue, F. Q. Bi, L. J. Zhai, T. Guo, J. R. Zhang, S. Y. Zhang, B. Z. Wang and J. L. Zhang, *ChemPlusChem*, 2019, **84**, 913; Y. N. Li, B. Z. Wang, Y. J. Shu, L. J. Zhai, S. Y. Zhang, F. Q. Bi and Y. C. Li, *Chin. Chem. Lett.*, 2017, **28**, 117; T. Guo, Z. J. Wang, H. Huo, W. Tang, Y. Zhu, F. Q. Bi and B. Z. Wang, *ChemistrySelect*, 2018, **3**, 11835; H. Li, F. Q. Zhao, B. Z. Wang, L. J. Zhai, W. P Lai and N. Liu, *RSC Adv.*, 2015, **5**, 21422; L. J. Zhai, X. Z. Fan, B. Z. Wang, F. Q. Bi, Y. N. Li and Y. L. Zhu, *RSC Adv.*, 2015, **5**, 57833.

2 L. J. Zhai, X. N. Qu, B. Z. Wang, F. Q. Bi, S. P. Chen, X. Z. Fan, G. Xie, Q. Wei and S. L. Gao, *ChemPlusChem*, 2016, **81**, 1156; Y. Tang, H. Gao, G. H. Imier, A. A. parrish and J. M. Shreeve, *RSC Adv.*, 2016, **94**, 91477.

3 N. V. Palysaeva, A. G. Gladyshkin, I. A. Vatsadze, K. Y. Suponitsky, D. E. Dmitrievd and A. B. Sheremetev, *Org. Chem. Front.*, 2019, **6**, 249; R. Haiges and K. O. Christe, *Dalton Trans.*, 2015, **44**, 10166; W. X. Wang, G. B. Cheng, H. L. Xiong and H. W. Yang, *New J. Chem.*, 2018, **42**, 2994; J. L. Zhang, Y. Z. Liu, J. Zhou, F. Q. Bi and B. Z. Wang, *ChemPlusChem*, 2019, **84**, 92; Q. Ma, Z. Lu, L. Liao, J. Huang, D. Liu, J. Li and G. Fan, *RSC Adv.*, 2017, **7**, 38844.

4 L. J. Zhai, F. Q. Bi, Y. F. Luo, N. X. Wang, J. L. Zhang and B. Z. Wang, *Sci. Rep.*, 2019, **9**, 4321; L. J. Zhai, F. Q. Bi, Y. F. Luo, L. Sun, H. Huo, J. C. Zhang, J. L. Zhang, B. Z. Wang and S. P. Chen, *Chem. Eng. J.*, 2019, DOI: 10.1016/j.cej.2019.123573.

5 A. TrzcinskiW, S. Cudziło, Z. Chyłek and L. Szymanczyk, *J. Hazard. Mater.*, 2008, **157**, 605.

6 A. Astrat'ev, D. Dashko and A. Stepanov, *New Trends in Research of Energetic Materials*, Czech Republic, 2011, p. 468; C. Yan, H. Yang, X. Qi, Y. Jin, K. Wang, T. Liu, J. Tian, F. Nie, G. Gang and Q. Zhang, *Chem. Commun.*, 2018, **54**, 9333.

7 H. Gao and J. M. Shreeve, *Angew. Chem., Int. Ed.*, 2015, **54**, 1.

8 T. M. Klapotke, B. Krumm, S. F. Rest and M. Suceska, *Z. Anorg. Allg. Chem.*, 2014, **640**, 84; V. V. Semenov, M. I. Kanischev, S. A. Shevelev and A. S. Kiselyov, *Tetrahedron*, 2009, **65**, 3441.

9 L. J. Zhai, B. Z. Wang, K. Z. Xu, H. Huo, N. Liu, Y. N. Li, H. Li, P. Lian and X. Z. Fan, *J. Energ. Mater.*, 2016, **34**, 92; O. A. Lukyanov, G. V. Pokhvisneva, T. V. Ternikova, N. I. Shlykova and M. E. Shagaeva, *Russ. Chem. Bull.*, 2011, **60**, 1703.

10 A. G. Orpen, L. Brammer, F. H. Allen, O. Kennard, D. G. Watson and R. Taylo, *J. Chem. Soc., Dalton Trans.*, 1989, **12**, S1; Y. Tang, H. Gao, L. A. Mitchell, D. A. Parrish and J. M. Shreeve, *Angew. Chem., Int. Ed.*, 2016, **128**, 3252; T. M. Klapotke, D. G. Piercey and J. Stierstorfer, *Dalton Trans.*, 2012, **41**, 9451.

11 Y. Oyumi, T. B. Brill and A. L. Rheingold, *J. Phys. Chem.*, 1985, **89**, 4824.

Open Access Article. Published on 24 March 2020. Downloaded on 5/11/2026 10:03:20 AM.
This article is licensed under a Creative Commons Attribution-NonCommercial 3.0 Unported Licence.

12 T. Lu and F. Chen, *J. Comput. Chem.*, 2012, **33**, 580; T. Lu and F. Chen, *J. Mol. Graphics Modell.*, 2012, **38**, 314.
13 D. Fischer, T. M. Klapötke and J. Stierstorfer, *Eur. J. Inorg. Chem.*, 2014, 5808; T. M. Klapötke, A. Nordheider and J. Stierstorfer, *New J. Chem.*, 2012, **36**, 1463; A. Hammerl, T. M. Klapötke and H. Nöth, *Propellants, Explos., Pyrotech.*, 2003, **28**, 165.
14 M. J. Frisch, G. W. Trucks, H. B. Schlegel, G. E. Scuseria, M. A. Robb, J. R. Cheeseman, J. A. Montgomery Jr, T. V. Reven, K. N. Kudin, J. C. Burant, J. M. Millam, S. S. Iyengar, J. Tomasi, V. Barone, B. Mennucci, M. Cossi, G. Scalmani, N. Rega, G. A. Petersson, H. Nakatsuji, M. Hada, M. Ehara, K. Toyota, R. Fukuda, J. Hasegawa, M. Ishida, T. Nakajima, Y. Honda, O. Kitao, H. Nakai, M. Klene, X. Li, J. E. Knox, H. P. Hratchian, J. B. Cross, V. Bakken, C. Adamo, J. Jaramillo, R. Gomperts, R. E. Stratmann, O. Yazyev, A. J. Austin, R. Cammi, C. Pomelli, J. W. Ochterski, P. Y. Ayala, K. Morokuma, G. A. Voth, P. Sal-vador, J. J. Dannenberg, V. G. Zakrzewski, S. Dapprich, A. D. Daniels, M. C. Strain, O. Farkas, D. K. Malick, A. D. Rabuck, K. Raghavachari, J. B. Foresman, J. V. Ortiz, Q. Cui, A. G. Ba-boul, S. Clifford, J. Cioslowski, B. B. Stefanov, G. Liu, A. Lia-shenko, P. Piskorz, I. Komaromi, R. L. Martin, D. J. Fox, T. Keith, M. A. Al-Laham, C. Y. Peng, A. Nanayakkara, M. Challacombe, P. M. W. Gill, B. Johnson, W. Chen, M. W. Wong, C. Gonzalez and J. A. Pople, *Gaussian*, Inc., Wallingford CT, 2009.
15 J. J. A. Montgomery, M. J. Frisch, J. W. Ochterski and G. A. Petersson, *J. Chem. Phys.*, 2000, **112**, 6532–6542; J. W. Ochterski, G. A. Petersson and J. A. Montgomery, *J. Chem. Phys.*, 1996, **104**, 2598–2619.
16 F. Trouton, *Philos. Mag.*, 1884, **18**, 54–57; M. S. Westwell, M. S. Searle, D. J. Wales and D. H. Williams, *J. Am. Chem. Soc.*, 1995, **117**, 5013–5015; Y. Zhang, D. A. Parrish and J. M. Shreeve, *J. Mater. Chem. A*, 2013, **1**, 585–593.
17 M. Suceska, *EXPLO5, Version 6.04*, 2017.
18 *Test methods according to the UN Recommendations on the Transport of Dangerous Goods, Manual of Tests and Criteria*, United Nations Publication, New York, 4th edn, 2003, 13.4.2 Test 3 (a) (ii) BAM Fall hammer, p. 75, 13.5.1 Test 3 (b) (i) BAM friction apparatus, p. 104.
19 Y. Qu and S. P. Babailov, *J. Mater. Chem. A*, 2018, **6**, 1915.
20 M. Sućeska, *Propellants, Explos., Pyrotech.*, 1991, **16**, 197.
21 T. K. R. Dennington and J. Millam, *GaussView 5, V5.0.8*, Semichem Inc., Shawnee Mission, 2009.
22 E. F. C. Byrd and B. M. Rice, *J. Chem. Phys.*, 2005, **110**, 1005–1013; L. A. Curtiss, K. Raghavachari, P. C. Redfern and J. A. Pople, *J. Chem. Phys.*, 1997, **106**, 1063–1079.

 This journal is © The Royal Society of Chemistry 2020